The contribution of synaptic depression to phase maintenance in a model rhythmic network

Y. Manor[1], A. Bose[2,3], V. Booth[3] and F. Nadim[2,3,4]

[1] Life Sciences Department and Zlotowski Center for Neurosciences
Ben-Gurion University of the Negev
Beer-Sheva, Israel 84105

[2] Department of Mathematical Sciences
New Jersey Institute of Technology, Newark, NJ 07102

[3] Center for Applied Mathematics and Statistics
New Jersey Institute of Technology, Newark, NJ 07102

[4] Department of Biological Sciences
Rutgers University, Newark, NJ 07102

CAMS Report 0203-14, Spring 2003

Center for Applied Mathematics and Statistics

NJIT

The contribution of synaptic depression to phase maintenance in a model rhythmic network

Yair Manor

Life Sciences Department and Zlotowski Center for Neurosciences, Ben-Gurion University of the Negev, Beer-Sheva, Israel 84105. yairman@bgumail.bgu.ac.il

Amitabha Bose

Department of Mathematical Sciences, New Jersey Institute of Technology, Newark, NJ 07102. bose@m.njit.edu

Victoria Booth

Center for Applied Mathematics and Statistics, New Jersey Institute of Technology, Newark, NJ 07102. victoria_booth@yahoo.com

Farzan Nadim

Department of Mathematical Sciences, New Jersey Institute of Technology and Department of Biological Sciences, Rutgers University, Newark, NJ 07102. farzan@njit.edu

Running head: Synaptic depression promotes phase invariance

Correspondence: Yair Manor, Life Sciences Dept., Ben-Gurion University of the Negev, P.O. Box 653, Beer-Sheva, Israel 84105. yairman@bgumail.bgu.ac.il. Phone (+972) 8-646-1353. Fax (+972) 8-647-9214.

Keywords: Phase constancy, Synaptic dynamics, Central Pattern Generation, Oscillations

Abstract

In many rhythmic neuronal networks that operate in a wide range of frequencies, the time of neuronal firing relative to the cycle period (the phase) is invariant. This invariance suggests that, when frequency changes, firing time is precisely adjusted, either by intrinsic or synaptic mechanisms. We study the maintenance of phase in a computational model in which an oscillator neuron (O) inhibits a follower neuron (F) by comparing the dependency of phase on cycle period in two cases: when the inhibitory synapse is depressing and when it is non-depressing. Of the numerous ways of changing the cycle period, we focus on three cases where either the duration of the active state, the inactive state, or the duty cycle of O remains constant. In each case, we measure the phase at which F fires with respect to the onset of firing in O. With a non-depressing synapse this phase is generally a monotonic function of cycle period, except in a small parameter range in the case of the constant inactive duration. In contrast, with a depressing synapse, there is always a parameter regime in which phase is a cubic function of cycle period: it decreases at short cycle periods, increases in an intermediate range and decreases at long cycle periods. This complex shape for the phase-period relationship arises because of the interaction between synaptic dynamics and intrinsic properties of the postsynaptic neuron. By choosing appropriate parameters, the cubic shape of the phase-period curve results in a small variation in phase for a large interval of periods. Consequently, we find that although a depressing synapse does not produce perfect phase maintenance, it is generally superior to a non-depressing synapse in promoting a constant phase difference.

Introduction

Neuronal oscillations have been implicated in cognitive functions (Eckhorn et al. 1988; Fries et al. 2001; Gray et al. 1989; Rodriguez et al. 1999), in various sensory states (Laurent et al. 1996; Patel and Baladan 2000; Perez-Orive et al. 2002) and in the production of motor patterns (Grillner et al. 2000; Marder 2000; Nusbaum and Beenhakker 2002). In many cases, such neuronal networks produce rhythmic activity over a wide range of frequencies (Marder and Calabrese 1996). The output of a rhythmic network is defined by the frequency dependence of the activity of individual neurons, or groups of neurons. For instance, the activity of different neurons may be separated by a fixed time latency, despite wide changes in frequency (Ahissar et al. 2000; Bartos et al. 1999; Faulkes and Paul 1998). Often, however, rather than a constant latency neurons maintain a constant *phase* difference (DiCaprio et al. 1997; Friesen and Pearce 1993; Grillner 1981; O'Keefe and Recce 1993; Young 1975), where the phase difference is the ratio of latency and cycle period. In other cases, when frequency is changed neurons in the network show differences in activity times that range between constant latency and constant phase (Davis 1969; Fischer et al. 2001; Grillner 1981; Hooper 1997a; 1997b; Pearson and Iles 1970).

Nowhere is the importance of phase adjustment more obvious than in rhythmic motor systems, which operate in a wide range of frequencies (Brodin et al. 1985; Marder and Calabrese 1996; Mercier and Wilkens 1984; Skinner and Mulloney 1998), and where mechanical restrictions dictate that the pattern in muscle activity should be adjusted in

accordance to speed of movement. In the crab ventilatory system, for instance, phase constancy is necessary to produce a smooth and coordinated movement of the ventilatory pump (DiCaprio et al. 1997). In lamprey and other aquatic organisms propelled by undulatory locomotion, fixed phase lags between consecutive segments guarantee that the rostro-caudal axis of the body forms exactly one wavelength. This ensures the minimization of lateral thrust and the optimization of swimming at all possible speeds (Grillner 1974; Sigvardt 1981).

Despite its importance in central pattern generation, the mechanisms underlying phase constancy are not well understood. Except for special cases such as in-phase and anti-phase oscillations (Abarbanel et al. 1996; Schweighofer et al. 1999; Sherman and Rinzel 1992), there is no obvious general mechanism that explains how phase differences could be maintained across different cycle frequencies. Several studies have addressed the problem of phase maintenance in chains of coupled oscillators, and have proposed that the mechanism underlying phase constancy is embedded within the circuitry. In Williams (1992), for example, the synapses that make up a unit oscillator are repeated in neighboring segments, albeit with a reduced synaptic strength. In Skinner and Mulloney (1998), in each segment one neuron makes equal excitatory and inhibitory connections to two identical neurons in the previous segment. In both works, even though phase constancy was demonstrated, the essence of the mechanism remains unclear.

In this work, we propose a novel mechanism involving short-term synaptic depression to create phase maintenance between neurons in rhythmic networks. We consider a simple

model network consisting of an oscillatory neuron that has an inhibitory synapse onto a follower neuron. The mechanism is based on the simple idea that the latency of firing in the postsynaptic cell is directly affected by the synaptic strength. In a non-depressing synapse, the strength and time course of the synapse are independent of cycle frequency. In contrast, when the synapse is depressing, synaptic strength varies with cycle frequency, allowing postsynaptic latency to vary as well. With the correct choice of synaptic dynamics, we show that it is possible to vary the postsynaptic latency in a way that is approximately proportional to the change in cycle frequency, thereby allowing the phase to be relatively well maintained.

We have intentionally chosen a very simple oscillator-follower model to illustrate our proposed mechanism for phase maintenance. In spite of the simplicity of this model, the explanation of how a depressing synapse contributes to maintain phase is surprisingly complicated. As we will show, this complexity arises because of the interaction between synaptic dynamics and intrinsic properties of the postsynaptic neuron. At certain cycle periods, the latency is determined by the intrinsic properties alone, whereas in other cycle periods it is mostly affected by the synaptic dynamics. In principle, there can be numerous ways in which cycle period of an oscillatory system can change. We explore in detail three cases, where cycle period is varied while preserving the duration of the active state, the duration of the inactive state or both durations proportionally. Despite their simple nature, these three representative ways of changing the cycle period provide results that are insightful for the general case. Indeed, in all three cases synaptic depression provides a degree of flexibility that can be used to automatically adjust the

time difference between the activities of the two neurons, such that their phase difference is approximately maintained. Although a depressing synapse does not produce perfect phase maintenance, we show that it is generally superior to a non-depressing synapse in promoting a constant phase difference.

Materials and Methods

The circuit consists of an oscillator neuron (O) and a follower neuron (F) coupled with an inhibitory synapse from O to F. In this study we focus only on the effects of changing the period of the oscillator O on the activity of the follower cell F. Thus, for simplicity, O is modeled as a square wave oscillator that steps from a low voltage of -50 mV (the inactive state) to a high voltage of +50 mV (the active state). We stress that the results of this study do not depend on the specific implementation of the oscillator. For example, when we used Morris-Lecar equations to model the oscillator, we obtained similar results (not shown).

The durations of the active and inactive states of O are defined as T_A and T_I, respectively. The cycle period P is equal to $T_A + T_I$ (Fig 1, bottom trace). In this study we consider three ways of changing P: (1) The duration T_I of the non-active state of O varies and the duration T_A of the active state of O remains constant (T_A = 250 ms in Results). (2) Both T_I and T_A vary such that the ratio T_A/P (the duty cycle DC) remains constant (DC = 0.3 in Results). (3) T_I remains constant and T_A varies (T_I = 750 ms in Results).

We now describe the model of the follower neuron F and the synapse from O to F. For each case of changing *P,* we hereafter refer to the model with the parameter values given below as the "reference model". When noted, the reference model will be changed to assess the dependence of our model on parameters (see Results).

The cellular model

The follower cell F is modeled with standard current balance equations based on the Morris-Lecar model (Morris and Lecar 1981). The cell includes a fast activating conductance with high equilibrium potential (the "calcium" conductance), a slow activating conductance with low equilibrium potential (the "potassium" conductance) and a non voltage-dependent conductance (the "leak" conductance):

$$dV_F/dt = -\ \bar{g}_{Ca}\ m_\infty(V_F)\ (V_F - E_{Ca}) -\ \bar{g}_K\ w_F\ (V_F - E_K) - g_L\ (V_F - E_L) - I_{syn} + I_{ext}$$

$$dw_F/dt = (w_\infty(V_F) - w_F)\ /\ \tau_F$$

where V_F is the membrane potential and w_F governs the gating of the potassium conductance. The maximal conductances are (in mS/cm^2): $\bar{g}_{Ca} = 0.3$, $\bar{g}_K = 0.6$ and $g_L = 0.15$; the reversal potentials are (in mV): $E_{Ca} = 100$, $E_K = -70$ and $E_L = -50$; the steady state activation functions are $m_\infty(V_F) = 0.5\ (1 + \tanh((V_F\ - 1)/14.5)$ for the calcium conductance, and $w_\infty(V_F) = 0.5\ (1 + \tanh((V_F\ - 20)/15)$ for the potassium conductance; the applied current $I_{ext,}$ is 7.5 μA/cm^2 . The parameter τ_F is equal to 150 ms in the constant T_A case and 100 ms in the other two cases. With these parameters, F is a quiescent neuron with a high voltage equilibrium point.

The synaptic model

The current balance equation for F includes an additional term that represents the synaptic current from O to F:

$$I_{syn} = \bar{g}_{syn}\, s\, (V_F - E_{syn}) \qquad (2)$$

where the synaptic reversal potential E_{syn} is -70 mV, and the maximal synaptic conductance $\bar{g}_{syn}$ (in mS/cm^2) is: 0.185 in the constant T_A case, 0.22 in the constant *DC* case and 0.35 in the constant T_I case.

The gating variable *s* represents the fraction of open synaptic channels. When the synapse is modeled as a depressing synapse, the value of *s* depends on a depression variable *d* (Bose et al. 2001). Figure 1 shows time traces of the postsynaptic voltage V_F (top trace), *s* (thick, middle trace) and *d* (thin, middle trace). At the onset time of the active state of O, *s* is set to the value of *d*. Except for this single time point, *s* decays to 0 in two steps: during the active state of O (black bars, bottom trace), *s* decays with a slow time constant τ_η. In our study, we set τ_η=25 s, so that *s* remains essentially constant for the duration of the active state; during the non-active state of O (between black bars, bottom trace), *s* decays with a time constant τ_κ. The value of τ_κ is 1.5 s in the constant T_A case, 0.5 s in the constant *DC* case and 0.3 s in the constant T_I case. Hence, except for the single time point where *s* is set to the value of *d*, the dynamics of *s* are governed by the following equation:

$$ds/dt = -(s/\tau_\kappa)\, H_\infty(V_\theta - V_O) - (s/\tau_\eta)\, H_\infty(V_O - V_\theta) \qquad (3)$$

where H_∞ is the Heaviside function (0 when the argument is negative, 1 when it is positive), V_O is the membrane potential of O and V_θ = 0 mV.

The variable d represents the depression state of the synapse. It evolves independently of s, decreasing towards 0 with time constant τ_β when $V_O > V_\theta$, and recovering towards 1 with time constant τ_α when $V_O < V_\theta$:

$$\mathrm{d}d/\mathrm{d}t = ((1-d)/\tau_\alpha) H_\infty(V_\theta - V_O) - (d/\tau_\beta) H_\infty(V_O - V_\theta) \qquad (4)$$

where τ_α= 3 s; τ_β = 1.5 s for the constant T_A case and 0.5 s for the other two cases. For a depressing synapse the peak strength of the synaptic current depends on the peak value of d during the cycle. We refer to the model with the parameter values given above for each of the three cases considered as the reference model for each case.

To make a synapse non-depressing, we uncouple the dynamics of s on d: at the onset time of the active state in O we set s to a constant value. All other components in the dynamics of s are unchanged. We can tune a non-depressing synapse to have dynamics identical to a depressing synapse at a specific cycle period by setting s to the peak value of s (s_{peak}) for that specific case of the depressing synapse.

We hereafter define $g = \bar{g}_{syn}\, s$ to refer to the (actual) synaptic conductance. Note that if the synaptic conductance is too large, activity in F is suppressed. Thus, a necessary, but not sufficient, condition for F to become active is that g is less than some threshold value g^*. The conductance g may be less than g^* if either $\bar{g}_{syn}$ is small (the inhibition is weak) or (for a large $\bar{g}_{syn}$, i.e. a strong inhibition) s decays to a sufficiently small value. In this latter case, if lasts long enough, the condition $g < g^*$ becomes a sufficient condition for the transition to the active state. We further define g_{peak} as the value of g at the onset of O activity, i.e. at the instant that s is set to the value of d. Since s decays at all other times,

g_{peak} is the peak value of g reached during a cycle. Depending on the cycle period, g_{peak} may be greater than or less than g^*. In the former case, the synapse is defined as weak; it is strong in the latter case.

Definition of time interval and phase

For the analysis of the effects of the depressing synapse on the timing of F firing, we arbitrarily define the onset of firing of a neuron as the time at which the voltage of this neuron increases past V_θ (0 mV in our study) The cycle period P is defined by the interval between consecutive onsets of firing in neuron O. Δt is defined as the time interval between the onset of firing in O and the subsequent onset of firing in F. The phase (ϕ) of F firing is defined as $\Delta t/P$. Thus, ϕ ranges between 0 and 1, with both extremes corresponding to the case where O and F start their active states at the same time. Whenever P is changed, we allow the system to equilibrate before we measure the values of Δt and ϕ.

All numerical simulations were done with the software XPPAUT (Ermentrout 2002).

Results

In this study we examine how the existence of synaptic depression affects the activity time (Δt) of follower neurons when the cycle period (P) changes. Δt is a direct function of the synaptic strength. When the synapse is non-depressing, the synaptic strength is independent of P. In contrast, with a depressing synapse the synaptic strength changes as a function of P. Hence, a depressing and a non-depressing synapse affect the activity time of the follower neuron in different ways. Figure 2 illustrates this fact by comparing

the activity of a follower neuron with a depressing and non-depressing synapse, for three different values of P. Here, when the synapse was non-depressing Δt was fixed for all three values of P; with a depressing synapse, Δt was larger for larger P values. If the increase in Δt was proportional to the increase in P, the phase ($\phi = \Delta t/P$) would be perfectly maintained. This example shows that, under appropriate conditions, the dependence of Δt on P could provide a mechanism for keeping phase approximately constant, across different cycle periods.

In general, how Δt changes with P depends, among other things, on how P is changed. Of the numerous ways to change P, we considered three different cases. These cases are shown in Fig. 3 and are labeled the constant T_A case, the constant DC case and the constant T_I case. In the constant T_A (T_I) case, we varied P by modifying only T_I (T_A). In the constant DC case, both T_A and T_I were proportionally varied such that the duty cycle remained constant. There are, of course, other ways to vary P. However, we believe that these three extreme cases are good representatives of the effect of a depressing synapse when P is arbitrarily changed.

Our results are divided in three sections. First, we describe how the synaptic conductance g changes as a function of period for the constant T_A, DC and T_I cases. This is followed by a detailed explanation of the dependence of Δt and phase on cycle period in these three cases. Finally, we give a description of how various biophysical model parameters affect the dependency of phase on cycle period.

The dependence of synaptic conductance on cycle period

The oscillatory activity of O dictates an oscillatory time course for the synaptic conductance g ($= \bar{g}_{syn}\, s$). At the onset of O activity, the synaptic conductance g is at its peak value $g_{peak.}$ The synaptic conductance then decays, first with time constant τ_η (when O is active) and then with time constant τ_κ (when O is inactive; see Fig. 1). We define g_{jump} as the value of g immediately before the onset of F activity. Δt is the time during which g decays from g_{peak} to g_{jump}. Analytical derivations for g_{peak} and Δt are provided in the Appendix. An analytical expression for g_{jump} depends on the intrinsic properties of F and will not be derived here. However, we will show that for a range of P values, g_{jump} is constant.

The primary effect of synaptic depression was to change the value of g_{peak}. The following equation defines g_{peak}, regardless of how P is changed (see Appendix):

$$g_{peak} = \bar{g}_{syn}\,(1 - \exp(-T_I/\tau_\alpha)) \,/\, (1 - \exp(-T_I/\tau_\alpha)\exp(-T_A/\tau_\beta)). \qquad (5)$$

Equation (5) shows that g_{peak} depends not only on P ($= T_I + T_A$), but also on the time constants of recovery (τ_α) and depression (τ_β) and the maximal conductance $\bar{g}_{syn}$.

Figure 4 shows how g_{peak} and g_{jump} depended on P for the three different cases, when the synapse was depressing. The effect of the synapse on F depended on the relationship of g_{peak} and g_{jump} to g^*, the synaptic conductance below which the synapse was too weak to keep F inactive (see Methods). In general, two factors can determine the firing time of F:

the intrinsic properties of F and the synaptic dynamics. The strength of the synapse determined which of these two factors affected the firing time of F. For example, if the synapse was recovered enough so that g_{peak} was larger than g^* and g_{jump} was equal to g^*, then the firing time of F was completely determined by the synapse. In this case, the necessary condition for F firing ($g_{jump} \leq g^*$) became a sufficient condition. On the other hand, if the synapse was depressed and g_{peak} was smaller than g^*, the firing of F was mainly determined by its intrinsic properties since the synapse was too weak to greatly affect it. In this case, g_{jump} was not fixed: its variation with P resulted from the variation of g_{peak} with P.

In Fig. 4A, V_F and g are shown for the constant T_A case when P=500, 1000 and 2000 ms. At P=500 ms, both g_{peak} and g_{jump} were less than the value g^* (dotted horizontal line). At P=1000 and 2000 ms, g_{peak} was larger than g^* whereas g_{jump} was equal to g^*. Figure 4B shows the dependencies of g_{peak} and g_{jump} on P for a continuous range of P values. Because P was increased by increasing T_I, as P increased the synapse had more time to recover from depression, and thus g_{peak} increased (as can also be seen directly from Equation 5). For P < 500 ms the synapse was too weak to remove F from its high voltage fixed point and F displayed no rhythmic activity (not shown). For P values larger than 500 ms, both g_{peak} and g_{jump} increased with P. For P values smaller than 750 ms, g_{peak} was smaller than g^*: the synapse was weak and the firing of F was mainly affected by the intrinsic properties of F. For P values larger than 750 ms but smaller than 1250 ms, g_{peak} was larger than g^*, but g_{jump} was smaller than g*. In this range, the synapse affected the firing time of F together with the intrinsic properties of F. When P was larger than 1250

ms, g_{jump} reached the constant value g^* and the firing of F was completely determined by the synapse.

Figures 4C and D show the corresponding situation for the constant *DC* case. This case is similar to the constant T_A case in the qualitative dependencies of g_{peak} and g_{jump} on *P*. Note that g_{peak} and g_{jump} increased with *P,* and this result was independent of the choice of time constants of recovery and depression (not shown). Here the synapse completely determined the firing time of F ($g_{peak} > g^*$ and $g_{jump} = g^*$) when *P* was larger than 2500 ms. This value is relatively large, compared to the constant T_A case (where the synapse completely determined the firing time of F when P was larger than 1250 ms). This is because, here, *P* was increased by increasing both T_A and T_I. Hence, not only the recovery from depression increased when P increased, but also the extent of depression.

Figures 4E and F show the situation for the T_I constant case. Here the dependencies of g_{peak} and g_{jump} on *P* were opposite to those found in the previous two cases. Both g_{peak} and g_{jump} *decreased* when *P* increased. This is because *P* was increased by increasing T_A only, and a larger value of T_A produced a greater depression of the synapse and thus a smaller value of g_{peak}. This can also be seen directly from Equation (5). In this case, the two conditions for which the synapse totally determined the firing time of F, $g_{peak} > g^*$ and $g_{jump} = g^*$, were obtained for *P* values *smaller* than 1750 ms. For *P* values larger than 1750 ms, g_{jump} decreased from g* as *P* increased, and the firing time of F was mostly determined by its intrinsic properties (the synapse was too depressed).

Analytical description of Δt

In this section we show how the values of g_{peak} and g_{jump} determine Δt. Since Δt is determined by the rates at which the conductance decays from g_{peak} to g_{jump}, the following equation describes the dependence of Δt on model parameters for sufficiently large $\bar{g}_{syn}$ (see also Appendix):

$$\Delta t = \tau_\kappa \cdot \ln(g_{peak} / g_{jump}) + T_A (1 - \tau_\kappa/\tau_\eta). \qquad (6)$$

In general, both Δt and g_{jump} are values that are *a priori* not known. Hence, in the general case this equation cannot be used to compute Δt. When the O to F synapse is weak, the time of F firing is largely controlled by its intrinsic properties. Thus, at this time the synaptic conductance g_{jump} is mostly determined by the intrinsic dynamics of F. In this case, Equation (6) cannot be used to compute Δt without resolving the dependence of g_{jump} on F dynamics. However, with a stronger O to F synapse, g_{jump} becomes equal to the constant value g*, as seen in Fig. 4, and hence:

$$\Delta t = \tau_\kappa \cdot \ln(g_{peak} / g^*) + T_A (1 - \tau_\kappa/\tau_\eta). \qquad (7)$$

In this case, all terms on the right hand side of Equation (7) are known and Δt can be analytically calculated. Equations (6-7) apply when the synapse is recovered enough to determine the firing time of F, i.e., to the constant T_A and *DC* cases when P is large and to the constant T_I case when P is small. For simplicity, in our model we assumed that τ_η is

large relative to τ_K, such that during the active state of O the synaptic decay is minimal. In this case, Equation (7) can be approximated by the following equation:

$$\Delta t = \tau_K \ln(g_{peak} / g^*) + T_A \qquad (8)$$

We now describe in detail the dependence of Δt and phase of F firing ($\phi = \Delta t/P$) on P, in each of these three cases.

The dependence of Δt and phase on period in the constant T_A case

As we saw from Fig. 4 A&B, increasing the period by keeping T_A constant allowed the synapse to recover from depression without changing the extent of depression. In Fig. 5A we compare the activity of F when the synapse is non-depressing and depressing at P= 1000 and P=2000 ms. The top and bottom traces show the membrane potential of F and the synaptic variable g, respectively. For the sake of comparison, we tuned the strength of the non-depressing synapse such that its g_{peak} value was identical to the g_{peak} value when the synapse was depressing and P was 1000 ms (see Methods). Thus, at P = 1000 ms, the time courses of g and V_F were identical for the depressing and the non-depressing synapses (traces are superimposed, Fig. 5A left traces). At P = 2000 ms, in the non-depressing case g_{peak} was 120 μS/cm^2, identical to its value at P = 1000 ms (horizontal dotted line). Thus, Δt was unchanged. In contrast, in the depressing case, g_{peak} was 155 μS/cm^2, since the synapse recovered more from depression. This caused Δt to increase almost 1.5-fold.

Figure 5B shows the relationship between P and Δt (computed numerically) for the depressing (black) and non-depressing (blue) cases. To compare the two cases, the parameter $\bar{g}_{syn}$ for the non-depressing synapse was chosen such that ϕ=1 at P = 500 ms (the smallest P value that sustained a rhythm for F in the depressing case). The red line represents an idealized relationship in which phase is perfectly maintained at 0.643. Note that the depressing synapse case remained close to phase constancy for a large range of periods from P =500 to P =1200 ms.

Figure 5C plots ϕ as a function of P. The black, blue and red curves represent the depressing synapse, non-depressing synapse and idealized constant phase. In the case of a depressing synapse, the curve was cubic shaped with a local minimum at the point (P_1, ϕ_1) and a local maximum at (P_2, ϕ_2). In the non-depressing case, Δt was constant in this case and hence ϕ monotonically decreased like 1/P. Consequently, in the 1 sec interval between P = 500 and 1500 ms (marked by the vertical dotted lines in Fig. 5C), the change in phase for the depressing case (0.063) was much less than that of the non-depressing case (0.668).

In the depressing case, the cubic shape of ϕ vs. P was obtained because Δt was controlled by different mechanisms in different ranges of P values. With small P values ($P < P_1$), the synapse was largely depressed and hence Δt was mostly determined by the intrinsic dynamics of F. Because these intrinsic dynamics did not change with P, Δt was almost constant and thus ϕ behaved like 1/P. For $P > P_1$, the synapse increasingly contributed

to Δt because in this range of P values, the synapse increasingly recovered from depression. Between $P=P_1$ and $P=P_2$, ϕ increased because Δt increased more rapidly than P (Fig. 5C). This was due to the choice of synaptic parameters, in particular the fact that the synaptic decay τ_K was much slower than the intrinsic dynamics of F (τ_F). To understand the existence of the local maximum point at (P_2, ϕ_2), consider the situation when P was very large. In this case, the synapse was maximally recovering and g_{peak} and g_{jump} approached constant values ($\bar{g}_{syn}$ and g^* respectively), hence Δt approached a constant value. Hence, for large P values ϕ decreased like $1/P$. The increase and then decrease of ϕ, at intermediate and then large P values, imply the existence of a local maximum for ϕ.

The dependence of Δt and phase on period in the constant DC case

In contrast to the constant T_A case, when period was increased by keeping DC constant, both the recovery from depression and the extent of depression increased. Nevertheless, the effect of the depressing synapse in the constant DC case was qualitatively similar to the constant T_A case, because the dependence of g_{peak} and g_{jump} on P was similar in these two cases (Fig. 4 B & D). Figure 6A compares the activity of F when the synapse was non-depressing (dotted traces) and depressing (solid traces) at P=1000 and P=2000 ms. The description of this figure is similar to that of Fig. 5A.

It is important to emphasize that, in the constant DC case, the O to F synapse could affect the activity of F in two distinct ways depending on whether $\bar{g}_{syn}$ is smaller or larger than

g^*. This is true whether the synapse is depressing or not. When the synapse is non-depressing, $\bar{g}_{syn} > g^*$ implies that F remains inhibited as long as O is active, independent of the period P. We shall refer to this case as the strong non-depressing synapse. In contrast, when $\bar{g}_{syn} < g^*$ (weak non-depressing synapse), F need not remain inhibited for the entire active state of O (see for example the P=2000 ms traces of Fig. 6A). The weak depressing synapse behaves essentially the same way as the weak non-depressing synapse. This is not true for a strong synapse ($\bar{g}_{syn} > g^*$). Thus, when discussing the effect of a depressing synapse below, we treat the case of a strong depressing synapse

Figures 6B & 6C, respectively, show the dependence of Δt and ϕ on P for a range of P values for a depressing synapse (black curve), a strong (green curve) and three weak (blue curves) non-depressing synapses. The idealized constant phase case is represented as red curves). In the case of the depressing synapse, at short and intermediate P values, the dependency of Δt (and ϕ) on P was similar to the constant T_A case. However, at large P values, the constant DC case was qualitatively different than the constant T_A case. As P was increased, Δt approached a constant value in the constant T_A case, while here it continued to increase linearly. To understand why, recall that in both the constant T_A and constant DC cases, F activity started at some time interval after the end of activity in O ($\Delta t = T_A + \delta t$ where δt is the time interval between the end of O activity and the beginning of F activity). At large P values, the synapse was maximally recovered and hence δt no longer changed as P continued to increase. Since, in the constant DC case, T_A increased linearly with P, so did Δt. Consequently, ϕ approached the value of DC (T_A/P). This

results directly from the definition of phase $\phi = \Delta t/P = (T_A + \delta t)/P$. At large P values, the term $\delta t/P$ became negligible.

The dependence of Δt on P was qualitatively different for the weak and strong non-depressing synapses. When the non-depressing synapse was strong (green curves in Figs. 6B and 6C), at all P values F started to fire at a fixed time after the end of activity in O. Thus, Δt was equal to $T_A + \delta t$ and δt was constant for all P values because it only depended on τ_K, the decay time constant of the synapse (which is independent of P). Hence, as P increased, Δt increased linearly and ϕ decayed towards the duty cycle DC. When the non-depressing synapse was weak (blue curves in Figs. 6B & 6C, with 1 denoting the weakest synapse), the effect of the synapse on Δt and ϕ was qualitatively different for small and large P values. With large P values Δt was constant, whereas it increased for small P values. The transition point between these two regions moved to larger P values when $\bar{g}_{syn}$ was increased (from 1 to 3). To explain the existence of these two regions, recall that with a weak non-depressing synapse, following the onset of inhibition, F depolarized according to its intrinsic dynamics. Since the synapse was not strong enough to keep F inactive indefinitely, when P was large enough, F eventually started its activity while O was still active. In this case, Δt was independent of P since it only depended on the dynamics of F. Hence, for large P values Δt was constant, and ϕ decayed to 0. On the other hand, when P was small, the intrinsic dynamics of F did not have sufficient time to enable it to become active before O stopped its activity. Therefore, just as in the case of a strong non-depressing synapse, Δt was equal to $T_A + \delta t$ for some interval δt. However, in contrast to the strong non-depressing synapse where δt was

fixed, here δt decreased with P. To explain this, note that δt is the time it took F to reach activity after the end of O activity. As such, when the synapse was weak, δt was determined primarily by the intrinsic properties of F. Since, as P (and thus T_A) increased, the membrane potential of F at the end of O activity became more depolarized, with larger P, F was closer to activity threshold and it took less time (δt) for F to reach activity after the end of O activity. Since the decrease of δt was small relative to the increase in T_A (because the depolarization of F was relatively slow), overall, the sum $T_A + \delta t$ increased as P increased. Note that the increase in Δt in this case was due only to the increase in T_A and was completely independent of changes in T_I. However, the increase in P was due to increases in both T_A and T_I, and as a result ϕ decreased with P.

Note that in the 1 sec interval marked by the vertical dotted lines, the change in phase for the depressing synapse (0.149) was less than any of the non-depressing cases (strong: 0.467; weak 1: 0.269, 2: 0.272, 3: 0.214).

The dependence of Δt and phase on period in the constant T_I case

In the constant T_I case, the time during which the synapse depressed, and hence the extent of synaptic depression, grew as P increased. Hence, the synapse was most relevant when P was small. Figure 7A shows the activity of F when the synapse was non-depressing (dotted lines) and depressing (solid lines) at P=1000 and P=2000 ms. With a depressing synapse, the activity of F began at a *later* time for P=1000 ms compared to P=2000 ms.

This was due to the fact that the conductance of the depressing synapse was smaller when P increased (bottom traces).

Figures 7B & 7C, respectively, show the dependence of Δt and ϕ on P for a range of P values for a depressing synapse (black curve), a strong (green curve) and three weak (blue curves) non-depressing synapses. The idealized constant phase cases are shown as red curves. In the depressing case, the dependence of Δt on P went through a clear transition from being dependent on the properties of the depressing synapse to being dependent on intrinsic properties of F. The transition occurred at the P value corresponding to the local maximum of the Δt vs. P curve (P=1450 ms). For P values below this transition point, the synapse was strong (g_{peak} was larger than g^*) and hence F could switch to its active state only after the end of activity in O. In this regime, $\Delta t = T_A + \delta t$, where δt is the time interval from the end of activity in O to the beginning of activity in F. Note that both T_A and δt changed as P was increased but in opposite directions. The time interval δt decreased because the synapse became more depressed, while T_A increased linearly with P (by definition of the constant T_I case). Since these two time intervals were determined by completely separate parameters, with our choice of reference parameters, Δt initially decreased and then increased. For P values above the transition point, the synapse became too weak ($g_{peak} < g^*$) to keep F silent while O is active, and hence F started to fire before the end of activity in O. Near the transition point, the synapse still had an effect in delaying F's firing, but this effect weakened as P was increased. Hence Δt decayed. At P values larger than 2700 ms, the synapse was totally depressed and the firing time of F was exclusively determined by the intrinsic

dynamics of F. As a result, Δt approached a constant value. The phase curve had a local minimum and a local maximum, but for entirely different reasons than in the constant T_A and *DC* cases. The local maximum of the phase curve occurred at the *P* value at the local maximum in Δt (Fig. 7B). For larger *P* values, Δt decreased to a constant value and ϕ decayed to 0. To explain the occurrence of the local minimum in ϕ, recall that for *P* values below the local maximum there were two competing effects on Δt. As *P* increased, Δt (and therefore ϕ) first decreased. With further increases in *P*, Δt increased rapidly, causing ϕ to increase as well. This resulted in a local minimum at low *P* values.

When the synapse was non-depressing, as for the constant DC case, the dependence of Δt (and hence of ϕ) on *P* was qualitatively different if the synapse was strong ($\bar{g}_{syn} > g^*$, green curve) or weak ($\bar{g}_{syn} < g^*$, blue curves). As in Fig. 6B, the weak non-depressing cases are numbered from 1 to 3, with 1 marking the weakest case. When the non-depressing synapse was strong, F started to fire at some fixed time interval after the end of activity in O. Hence $\Delta t = T_A + \delta t$, where T_A increased linearly with *P* and δt was constant (as in the strong non-depressing constant DC case). Hence Δt increased. Because $\phi = T_A/P + \delta t/P$, as *P* was increased the first term approached 1 while the second term approached 0. Thus ϕ increased towards 1.

The dependence of Δt on *P* for the weak non-depressing synapse was identical to the constant DC case, since the arguments presented for the constant DC case depended only on changes in T_A. In the present case, in the range of *P* values where Δt increased with *P,*

ϕ also increased. This increase occurred for the same reasons that ϕ increased in the strong non-depressing case. In contrast, for larger P values, where Δt was constant, ϕ decayed to 0.

As in the constant DC and TA cases, over a 1 sec interval (vertical dotted lines), the depressing case showed a smaller total variation of phase (0.292) compared to the strong non-depressing case (0.302). However, note that the weak non-depressing case gave a smaller variation in phase, compared to the depressing case (1: 0.094, 2: 0.118, 3: 0.213). These results suggest that, in this case, a weak non-depressing synapse performs better than a depressing synapse in promoting phase constancy. However, we emphasize that this exception only applies for weak synapses that can only produce small values in the phase of F. If phase needs to be maintained at larger values, as could occur in biological networks, then, in this case as well as in others, a depressing synapse is superior to a non-depressing synapse.

The dependence of the phase-period relationship on intrinsic and synaptic parameters when T_A is constant

In general, the shape of the ϕ vs. P curve was determined by the intrinsic properties of F (τ_F) when P was small and by the properties of the synapse (τ_α, τ_β, τ_κ and $\bar{g}_{syn}$) when P was large. Since these parameters were independent, the ϕ vs. P curve could be cubic-like, depending on the choice of these parameters. Moreover, each of these parameters played a distinct role in determining the value and location of the local maximum and minimum points of the ϕ vs. P curve. The effects of these parameters on the ϕ vs. P

curve are illustrated in Fig. 8. The effect of increasing τ_β was qualitatively equivalent to decreasing τ_α (not shown). For conciseness, we only show the effect of the latter parameter. In each panel, the thick curve shows the reference model.

The two synaptic parameters, $\bar{g}_{syn}$ and τ_α, both controlled the strength of the synapse directly. The effect of $\bar{g}_{syn}$ on synaptic strength was present across all periods. Increasing $\bar{g}_{syn}$ caused the ϕ vs. P curve to shift up (Fig. 8A). Decreasing the recovery parameter τ_α had a similar effect, although this effect was more diminished for sufficiently large P values, since at these P values the synapse was mostly recovered from depression (Fig. 8B). In both cases, at any particular P value, strengthening the synapse caused ϕ to increase because Δt increased. This can be explained by considering Equations (5) and (6). Indeed, Equation (6) shows that, for sufficiently large P values (when g_{jump} is fixed at g*) Δt is an increasing function of g_{peak}. g_{peak} itself increases when τ_α is decreased or $\bar{g}_{syn}$ is increased, as can be seen from Equation (5).

In Fig. 8A, the maximum value of ϕ moved to the left as $\bar{g}_{syn}$ increased. Near the maximum, we recall that ϕ was determined entirely by the properties of the synapse so that F would only jump to its active state when g decayed below g^*. Since the synaptic conductance g is equal to $s\,\bar{g}_{syn}$, when $\bar{g}_{syn}$ increased, g decayed below g^* at a lower value of s, i.e. at a smaller P value. Thus the synapse would become more relevant for determining the firing time of F at lower values of P, causing the ϕ vs. P curve to shift up and to the left. Similar trends occur in Fig. 8B, as τ_α decreased. For any fixed P value,

smaller values of τ_α (faster recovery) caused g to increase. Hence, at any fixed P value, g decayed below g^* at a lower value of s, when τ_α was smaller. Again, this happened for smaller values of P implying that, as τ_α was decreased, the ϕ vs. P curve shifted up and to the left.

Of the three synaptic parameters analyzed, τ_κ is the only one that is not directly related to synaptic depression. Recall that the main effect of depression is to change g_{peak}, whereas τ_κ affects the time spent between g_{peak} and g_{jump}, but not g_{peak} itself. At small values of P, where the synapse was weak, τ_κ had almost no effect on ϕ (Fig. 8C). However, for larger P, τ_κ was the predominant parameter in determining how long g had to decay to release F from the inhibition of O. Thus, at larger P values, changes in τ_κ had a large effect on Δt and consequently on ϕ. Increasing τ_κ increased the maximum phase and shifted it to the right. This can be explained using Equations (6-8), which show that a simultaneous increase in both P and τ_κ shifts the ϕ vs. P curve up and to the right. Since Δt increased with τ_κ, for fixed P, ϕ increased as well, thereby shifting up the curve. Alternatively, if ϕ remained fixed, an increase in τ_κ would result in an increase in Δt and therefore in P, thereby shifting the curve to the right.

At large P values, the intrinsic parameter τ_F did not have any effect on ϕ because the synapse was dominant in determining the firing time of F (Fig. 8D). The effect on ϕ was restricted to smaller P values, when the synapse was relatively weak. For such a fixed P

value, decreasing τ_F forced F to spend less time in the silent state, thereby decreasing Δt, and therefore ϕ.

As seen in Fig. 8, changing any of the parameters shown could remove the local minimum and maximum of the ϕ vs. P curve. An examination of the parameter ranges for which the ϕ vs. P curve decreased monotonically revealed that in these ranges, the effect of the intrinsic properties of F was dominant over the effect of the depressing synapse in determining ϕ. This shift in the dominance of the intrinsic versus synaptic effects was produced either through a change in the relative time courses of these two factors (Fig. 8C&D), or by weakening the synapse (Fig. 8A&B).

The dependence of the phase-period relationship on intrinsic and synaptic parameters when the DC is constant

Figure 9 shows the dependence of the ϕ vs P curve on parameters in the *DC* constant case. In principle, the different parameters affected the ϕ vs P curve in a way that was similar to the constant T_A case. There were some differences between the two cases that are worth pointing out. In Fig. 9A, as $\bar{g}_{syn}$ was decreased, the value of the local minimum of the phase curve decreased and shifted to the right. Recall that in the constant *DC* case, larger P means that there is not only a longer time for the synapse to recover, but also a longer time for it to depress. This can be seen in Fig. 4, where $g_{peak} > g^*$ at much larger values of P for the constant *DC* case compared to the constant T_A case. Thus, at smaller values of $\bar{g}_{syn}$, the range of P values for which the intrinsic properties of F determined phase became larger. However, despite the smaller value of $\bar{g}_{syn}$, as P was increased to

very large values, the synapse became sufficiently large and determined phase. A similar effect was seen by increasing τ_α (Fig. 9B). In both Figs. 9A and B, the cubic shape of the phase curve persisted when the synapse was weakened because, as *P* approached infinity, ϕ tended to the value of *DC* (0.3).

As in the case of constant T_A, in the constant *DC* case, τ_κ had minimal effects on ϕ at small *P* values (Fig. 9C) and τ_F had minimal effects on ϕ at large *P* values (Fig. 9D).

The dependence of the phase-period relationship on intrinsic and synaptic parameters when T_I is constant

In Fig. 10, we show the phase curves when parameters are varied in the constant T_I case. Just as in the previous two cases, strengthening of the synapse (by increasing $\bar{g}_{syn}$ in Fig. 10A or decreasing τ_α in Fig. 10B) had the expected effect of raising the ϕ *vs P* curves and shifting them to the right. Figures 10A&B also show that, if the synapse was sufficiently strong, it could determine the firing time of F at all *P* values. For example, when $\bar{g}_{syn}$ = 0.55 or τ_α =1500 ms, ϕ approached 1, and not 0, as *P* increased. Thus, at large *P* values, the ϕ *vs P* curve was similar to the one obtained in the case of a strong non-depressing synapse (see Fig. 7C).

Figure 10C shows the effect of τ_κ on the ϕ *vs P* curve. In this case, τ_κ had no effect on ϕ when *P* was larger than the local maximum. This is expected since, in the constant T_I case, the synapse was weak at large *P* values, and in this range ϕ was determined by the

intrinsic properties of F. Figure 10D shows the effect of changing τ_F on the phase curve. The effect of τ_F was most prominent at *P* values larger than the local maximum, where the synapse was weak. In contrast to the constant T_A and *DC* cases (Figs. 8D and 9D), where changes in τ_F had no effect on phase in the synaptically controlled range of *P* values, in the constant T_I case there was a small dependence on τ_F even at P values smaller than the local maximum, where the firing time of F was mostly affected by the synaptic dynamics. This small effect on the phase curve occurred because the larger values of τ_F were comparable to (the reference value of) τ_K. For these cases, both the synapse and the intrinsic properties of F determined ϕ.

Discussion

Despite its abundance in nervous systems, it is only recently that the functional roles of short-term synaptic dynamics in general and synaptic depression in particular are beginning to be understood. It has been proposed that synaptic depression could be used as a mechanism for automatic gain control (Abbott et al. 1997; Tsodyks and Markram 1997). Synaptic depression has also been implicated in directional selectivity (Chance et al. 1998), burst detection (Lisman 1997), network stability (Galaretta and Hestrin 1998; Varela et al. 1999), rhythmogenesis (Friesen 1994), network synchronization (Tsodyks et al. 2000) and interval and sequence determination (Buonomano 2000). A recent set of theoretical and experimental studies raised the possibility that synaptic depression could be implicated in network reconfiguration, by mediating the occurrence of multi-stable states (Bose et al. 2001; Manor and Nadim 2001; Nadim et al. 1999). The current work is an effort in the same direction. It proposes a novel function for synaptic depression.

The effect of synaptic depression on the phase-period relationship

In this work we developed a biophysical model, which demonstrates that synaptic depression can be employed as a mechanism from promoting phase constancy. Our model is not meant to reproduce the output of any particular biological network. Thus, the parameters of our model were chosen to elucidate the effect of synaptic depression on phase maintenance in different conditions. By adjusting the values of these parameters, this model can be used to simulate various biological systems, for example cases where synaptic dynamics range from milliseconds to hundreds of milliseconds (such as in synapses of the pyloric circuit, see Manor et al. (1997)), or circuits with fast tonic spiking rather than slow bursting neurons. In all these cases, the essence of the model is the same. It is based on the idea that depressing synapses are frequency-dependent: longer intervals of no activity in the presynaptic neuron allow more recovery of the depressing synapses. When cycle period is varied by changing either (or both) the active or inactive durations (T_A or T_I) of the oscillator activity, there is a range of cycle periods in which a depressing synapse maintains phase better than a non-depressing synapse.

An important result of our study is that it reveals how a synapse works together with the intrinsic properties of the postsynaptic cell to determine the firing latency. When the synapse is depressing, its strength depends on cycle period. Thus, at some range of cycle periods the synapse determines the phase, whereas in other ranges the intrinsic properties of the postsynaptic cell control the phase. This interplay between intrinsic and synaptic

properties expands the interval of periods over which phase of the postsynaptic cell can be maintained. Interestingly, our study suggests that this result is general and holds even when cycle period is changed in very different ways.

In the constant T_A case, when cycle period P increases the synapse becomes stronger and Δt increases as well. Consequently, with the appropriate choice of parameters and range of P values, Δt increases such that the relation between phase ϕ and P follows a cubic form. At low P values, the synapse is not effective in delaying F activity. The time delay Δt is affected by the synapse, but it is mainly determined by the intrinsic properties of F. Hence, for a particular increase in P, Δt increases as well, but to a smaller extent. Consequently, in this range ϕ decreases. At an intermediate range the synapse is strong enough and Δt is mostly affected by the dynamics of the synapse. Here an increase in P causes a larger change in Δt and ϕ increases. At very large P values (relative to the time constant of synaptic recovery) the synapse is fully recovered and Δt is constant, causing ϕ to decrease like $1/P$. The cubic form of this relationship defines a range of cycle periods for which the change in phase is relatively small, compared to a non-depressing synapse for which phase decreases like $1/P$ over the whole range of cycle periods.

In essence, the constant DC case is similar to the constant T_A case except that, at large P values, ϕ does not decay to 0 but approaches the value of DC. This is because, as P increases to very large values, Δt approaches to T_A plus some fixed value, since the synapse maximally recovers from depression.

The constant T_I case is less intuitive. Here the depressing synapse becomes *weaker* as P increases. In the range of small P values, the synapse is strong and its dynamics control the phase. In this range, there are two opposing effects on the phase-period relationship. On one hand, because P is increased by increasing T_A, as P increases, the activity of F is delayed. On the other hand, as P increases the synapse becomes more depressed and the activity of F is advanced. The competition between these two effects causes ϕ to first decrease and then increase at low and intermediate P values. At larger P values, the control of phase changes from a synaptic to an intrinsic mechanism, and ϕ decreases like $1/P$.

Inhibitory synapses that show depression promote phase maintenance better than synapses that are non-depressing

In all three cases examined the phase-period relationship shows a local minimum followed by a local maximum. This defines a range of cycle periods for which the change in ϕ is limited. A depressing synapse does not guarantee phase constancy. However, our model demonstrates that, with very different ways of changing cycle period, an inhibitory depressing synapse is generally better than a non-depressing synapse, in promoting phase constancy. The sole exception occurs in the weak non-depressing constant T_I case, where the change in phase is smaller than with a depressing synapse. However, we emphasize that changing P by increasing only T_A is a worst-case scenario where the synapse is never given a chance to increase its strength when P is increased. Indeed, in *any* situation where increasing P is accompanied with some degree of increase in T_I (no matter how T_A changes), our study demonstrates that a depressing synapse is superior to a non-

depressing synapse in maintaining phase. This can be seen directly from Equation (5), which shows that g_{peak} approaches 1 with increases in T_I, independent of how T_A may change. As a result, in such cases (which form the majority of cases) the dependence of g_{peak} and g_{jump} on P will be qualitatively similar to the constant T_A and constant DC cases, where we demonstrated that a depressing synapse is better at maintaining phase compared to a non-depressing synapse.

The exception mentioned above strengthens the rule, and this for several reasons. First, in biological networks the constant T_I case is not common, and changes in cycle period are generally accompanied with changes in T_I. An extreme example is a circuit where neurons are tonic spikers (as mentioned above, by changing the scales of intrinsic and synaptic dynamics our analysis can be extended to tonic spikers, rather than slow oscillators as studied here). In such cases, the spiking frequency is only determined by the duration of the interspike intervals, since the spike duration is generally fixed. Second, in uncommon cases where T_I remains fixed when cycle period changes, a non-depressing synapse could give better phase maintenance only if it is weak, and in this case the phase difference will be necessarily small. When a larger phase difference is required, our study shows that even in this peculiar case a depressing synapse gives better results for phase maintenance.

We emphasize that, in our model, the depressing synapse improves the phase maintenance in a restricted range of, and not across all, P values. However, biological networks also operate in a limited physiological range of cycle periods. In addition, our

analysis shows that phase maintenance could be improved by choosing model parameters such that the cubic portion of the phase-period curve becomes flatter and wider.

State-dependence of phase maintenance

Several studies have shown that the extent of phase maintenance could vary under different behavioral circumstances. In insect locomotion, for example, during walking movements the coupling between the leg joints is phase-constant. In contrast, during searching movements this relationship is lost (Fischer et al. 2001). In the crustacean pyloric circuit, it was found that some phases were almost perfectly maintained when the stomatogastric ganglion was isolated from the influence of anterior ganglia, whereas the same phases were maintained less well in intact preparations (Hooper 1997a). To reconcile the differences, this study suggested that neuromodulatory inputs could alter the degree to which different pyloric elements keep phase. If phase maintenance is indeed state-dependent, our model provides a simple explanation. We have shown that different parameters of the synaptic dynamics could alter the degree of phase maintenance. These parameters could be directly affected by neuromodulation and it is tempting to speculate that modulation of the synaptic dynamics could affect the degree to which phase is maintained among different elements of the network.

In addition, our model provides the possibility that a neuromodulator primes the network without having an immediate effect on the frequency or the phase of neurons. Instead, the neuromodulatory action comes into effect when frequency is changed. For instance, in the constant T_A or *DC* cases, a neuromodulator that increases the time constant (τ_κ) of

synaptic decay has almost no effect on phase when the cycle period *P* is short. However, as *P* is increased, the previous modification of $\tau_\kappa$can produce a dramatic effect on phase. This is especially useful when the network needs to change from one type of activity to another in multiple, successive steps. If two groups of neurons operate with constant phase difference in one behavior but not in the other, such a priming mechanism would allow the transition to occur at the appropriate stage with minimal transient effects.

Phase maintenance in more complex conditions

In this work we studied the effect of an inhibitory depressing synapse between an oscillator neuron and a follower cell in a simple feed-forward network. To focus on the effects of synaptic dynamics we modeled the cells with a minimal set of intrinsic properties. We are well aware that this circuit is greatly simplified. In biological networks, the presence of additional ionic conductances can interact with synaptic influences to determine the activity time of a neuron. For instance, an outward A current elicited by a post-inhibitory rebound could increase the delay of a bursting neuron (Harris-Warrick et al. 1995a; Harris-Warrick et al. 1995b; Swensen and Marder 2001). Such a current could work in concert with the synaptic mechanism described here, to increase the time delay as cycle period increases, thereby improving phase maintenance. Inward currents elicited by inhibition, such as an *h* current, may do the opposite. The relative timing of neuronal events could be greatly affected by modifications in the intrinsic and/or synaptic properties of neurons. For instance, a larger burst in the presynaptic neuron may increase the amount of transmitter release, thereby advancing (for an excitatory synapse) or delaying (for an inhibitory synapse) the onset of

postsynaptic activity. The occurrence of feedback connections adds a new level of complexity that is beyond the scope of this discussion.

Conclusions

We have shown that synaptic depression can contribute to maintain phase in an oscillatory network across a range of cycle periods. Although we focused on only three representative ways to change cycle period, the results obtained from these three cases are insightful for the general case. An important characteristic of this model is that the adjustment of timing is internal and automatic. It is not regulated by external factors such as neuromodulation, but results causally from the change in cycle period, through the interaction between intrinsic and synaptic dynamics within the network. It has been proposed that, in rhythmic networks, time delays are changed by neuromodulation (DiCaprio et al. 1997; Harris-Warrick et al. 1995b). However, neuromodulation is also the means for changing cycle period in such networks. Parsimonious considerations dictate that, when phase maintenance is required for proper network function, delays should be adjusted to preserve phase automatically, *independent* of the extrinsic input that forces the change in period. A built-in mechanism such as the one proposed in this work, in concert with extrinsic modulation, provides a simple strategy for coordination of neuronal timing with cycle period.

Appendix

Derivation of Equation (5)

Suppose neuron O becomes active at $t = 0$ with $d(0)= d_0$. When neuron O is active, $d' = -d/\tau_\beta$. Thus at $t = T_A$, $d(T_A)= d_0 \exp(-T_A/\tau_\beta)$. When neuron O is silent, $d' = (1 - d)/\tau_\alpha$ with initial condition $d(T_A) = d_0 \exp(-T_A/\tau_\beta)$. Solving this equation gives:

$$d(t) = 1 - (1 - d_0 \exp(-T_A/\tau_\beta)) \exp(-(t - T_A)/\tau_\alpha) \qquad \text{(A1)}$$

Due to the periodicity of O, we impose the condition $d(T_A+T_I) = d_0$ in equation (A1). Solving for d_0 using the fact that $g_{peak} = \bar{g}_{syn} d_0$, we obtain:

$$g_{peak} = \bar{g}_{syn} (1 - \exp(-T_I/\tau_\alpha)) / (1 - \exp(-T_I/\tau_\alpha) \exp(-T_A/\tau_\beta)). \qquad (5)$$

Derivation of Equation (6)

Suppose $t = 0$ is the onset of activity in neuron O. When neuron O is active, $g' = -g/\tau_\eta$ and $g(0)= g_{peak}$, implying that $g(T_A) = g_{peak} \exp(-T_A/\tau_\eta)$. When neuron O is silent, $g' = -g/\tau_\kappa$ with initial condition $g(T_A) = g_{peak} \exp(-T_A/\tau_\eta)$. Solving this equation yields:

$$g(t)= g_{peak} \exp(-T_A/\tau_\eta) \exp(-(t - T_A)/\tau_\kappa) \qquad \text{(A2)}$$

Imposing the condition $g(\Delta t) = g_{jump}$ in Equation (A2) and solving for Δt, we obtain:

$$\Delta t = \tau_\kappa \ln(g_{peak}/g_{jump}) + T_A (1 - \tau_\kappa/\tau_\eta). \qquad (6)$$

Note that if the synapse is weak and F becomes active prior to the end of the O activity, Equation (6) does not apply. In this case, Δt satisfies the following equation:

$$\Delta t = \tau_\eta \ln (g_{peak} / g_{jump}) \qquad \text{(A3)}$$

Acknowledgments

This research was supported by ISF 314/99-1 (YM), BSF 2001-039 (YM & FN), NSF DMS-9973230 (AB & VB) and NIH MH-60605 01A1 (FN).

References

Abarbanel HD, Huerta R, Rabinovich MI, Rulkov NF, Rowat PF, and Selverston AI. Synchronized action of synaptically coupled chaotic model neurons. *Neural Comput* 8: 1567-1602, 1996.

Abbott L, Sen K, Varela J, and Nelson S. Synaptic depression and cortical gain control. *Science* 275: 220-222, 1997.

Ahissar E, Sosnik R, and Haidarliu S. Transformation from temporal to rate coding in a somatosensory thalamocortical pathway. *Nature* 406: 302-306, 2000.

Bartos M, Manor Y, Nadim F, Marder E, and Nusbaum MP. Coordination of fast and slow rhythmic neuronal circuits. *J Neurosci* 19: 6650-6660, 1999.

Bose A, Manor Y, and Nadim F. Bistable oscillations arising from synaptic depression. *SIAM J App Math* 62: 706-727, 2001.

Brodin L, Grillner S, and Rovainen CM. N-Methyl-D-aspartate (NMDA), kainate and quisqualate receptors and the generation of fictive locomotion in the lamprey spinal cord. *Brain Res* 325: 302-306, 1985.

Buonomano D. Decoding Temporal Information: A Model Based on Short-Term Synaptic Plasticity. *J Neurosci* 20: 1129-1141, 2000.

Chance F, Nelson S, and Abbott L. Synaptic depression and the temporal response characteristics of V1 cells. *J Neurosci* 18: 4785-4799, 1998.

Davis WJ. The neural control of swimmeret beating in the lobster. *J Exp Biol* 50, 1969.

DiCaprio RA, Jordan G, and Hampton T. Maintenance of motor pattern phase relationships in the ventilatory system of the crab. *J Exp Biol* 200: 963-974, 1997.

Eckhorn R, Bauer R, Jordan W, Brosch M, Kruse W, Munk M, and Reitboeck HJ. Coherent oscillations: a mechanism of feature linking in the visual cortex? Multiple electrode and correlation analyses in the cat. *Biol Cyber* 60: 121-130, 1988.

Ermentrout B. *Simulating, Analyzing, and Animating Dynamical Systems: A Guide to Xppaut for Researchers and Students (Software, Environments, Tools)*. Philadelphia: SIAM, 2002.

Faulkes Z and Paul DH. Digging in sand crabs: coordination of joints in individual legs. *J Exp Biol* 201 (Pt 14): 2139-2149, 1998.

Fischer H, Schmidt J, Haas R, and Buschges A. Pattern generation for walking and searching movements of a stick insect leg. I. Coordination of motor activity. *J Neurophys* 85: 341-353, 2001.

Fries P, Reynolds J, Rorie A, and Desimone R. Modulation of oscillatory neuronal synchronization by selective visual attention. *Science* 291: 1560-1563, 2001.

Friesen WO. Reciprocal inhibition: a mechanism underlying oscillatory animal movements. *Neurosci Biobehav* 18: 547-553, 1994.

Friesen WO and Pearce RA. Mechanisms of intersegmental coordination in leech locomotion. *Sem Neurosci* 5: 41-47, 1993.

Galaretta M and Hestrin S. Frequency-dependent synaptic depression and the balance of excitation and inhibition in the neocortex. *Nature Neuroscience* 1: 587-593, 1998.

Gray CM, Konig P, Engel AK, and Singer W. Oscillatory responses in cat visual cortex exhibit inter-columnar synchronization which reflects global stimulus properties. *Nature* 338: 334-337, 1989.

Grillner S. Control of locomotion in bipeds, tetrapods and fish. In: *Handbook of Physiology, section 1, The Nervous system, vol II*, edited by V.B. B. Maryland: Waverly Press, 1981, p. 1179-1236.

Grillner S. On the generation of locomotion in the spinal dogfish. *Exp Brain Res* 20: 459-470, 1974.

Grillner S, Cangiano L, Hu G, Thompson R, Hill R, and Wallen P. The intrinsic function of a motor system--from ion channels to networks and behavior. *Brain Res* 886: 224-236, 2000.

Harris-Warrick RM, Coniglio LM, Barazangi N, Guckenheimer J, and Gueron S. Dopamine modulation of transient potassium current evokes phase shifts in a central pattern generator network. *J Neurosci* 15: 342-358, 1995a.

Harris-Warrick RM, Coniglio LM, Levini RM, Gueron S, and Guckenheimer J. Dopamine modulation of two subthreshold currents produces phase shifts in activity of an identified motoneuron. *J Neurophysiol* 74: 1404-1420, 1995b.

Hooper SL. Phase maintenance in the pyloric pattern of the lobster (*Panulirus interruptus*) stomatogastric ganglion. *J Comput Neurosci* 4: 191-205, 1997a.

Hooper SL. The pyloric pattern of the lobster (*Panulirus interruptus*) stomatogastric ganglion comprises two phase maintaining subsets. *J Comput Neurosci* 4: 207-219, 1997b.

Laurent G, Wehr M, and Davidowitz H. Temporal representations of odors in an olfactory network. *J Neurosci* 16: 3837-3847, 1996.

Lisman J. Bursts as a unit of neuronal information: making unreliable synapses reliable. *TINS* 20: 38-43, 1997.

Manor Y and Nadim F. Synaptic depression mediates bistability in neuronal networks with recurrent inhibitory connectivity. *J Neurosci* 21: 9460-9470, 2001.

Manor Y, Nadim F, Abbott LF, and Marder E. Temporal dynamics of graded synaptic transmission in the lobster stomatogastric ganglion. *J Neurosci* 17: 5610-5621, 1997.

Marder E. Motor pattern generation. *Curr Opin Neurobiol* 10: 691-698, 2000.

Marder E and Calabrese RL. Principles of rhythmic motor pattern generation. *Physiol Rev* 76: 687-717, 1996.

Mercier AJ and Wilkens JL. Analysis of the scaphognathite ventilatory pump in the shore crab *Carcinus maenas*. I. Work and power. *J Exp Biol* 113: 55-68, 1984.

Morris C and Lecar H. Voltage oscillations in the barnacle giant muscle fiber. *Biophys J* 35: 193-213, 1981.

Nadim F, Manor Y, Kopell N, and Marder E. Synaptic depression creates a switch that controls the frequency of an oscillatory circuit. *Proc Natl Acad Sci USA* 96: 1-6, 1999.

Nusbaum MP and Beenhakker MP. A small-systems approach to motor pattern generation. *Nature* 417: 343-350, 2002.

O'Keefe J and Recce ML. Phase relationship between hippocampal place units and the EEG theta rhythm. *Hippocampus* 3: 317-330, 1993.

Patel AD and Baladan E. Temporal patterns of human cortical activity reflect tone sequence structure. *Nature* 404: 80-84, 2000.

Pearson KG and Iles JF. Discharge patterns of coxal levator and depressor motoneurones of the cockroach, *Periplaneta americana. J Exp Biol* 52: 139-165, 1970.

Perez-Orive J, Mazor O, Turner GC, Cassenaer S, Wilson RI, and Laurent G. Oscillations and sparsening of odor representations in the mushroom body. *Science* 297: 359-365, 2002.

Rodriguez E, George N, Lachaux J-P, Martinerie J, Renault B, and Varela FJ. Perception's shadow: long-distance synchronization of human brain activity. *Nature* 397: 430-433, 1999.

Schweighofer N, Doya K, and Kawato M. Electrophysiological properties of inferior olive neurons: A compartmental model. *J Neurophysiol* 82: 804-817, 1999.

Sherman A and Rinzel J. Rhythmogenic effects of weak electrotonic coupling in neuronal models. *ProcNatl Acad Sci (USA)* 89: 2471-2474, 1992.

Sigvardt K. A. Spinal mechanisms in the control of lamprey swimming. *Am Zool* 29: 19-35, 1981.

Skinner FK and Mulloney B. Intersegmental coordination of limb movements during locomotion: mathematical models predicts circuits that drive swimmeret beating. *J Neurosci* 18: 3831-3842, 1998.

Swensen AM and Marder E. Multiple peptides converge to activate the same voltage-dependent current in a central pattern-generating circuit. *J Neurosci* 20: 6752-6759, 2001.

Tsodyks M and Markram H. The neural code between neocortical pyramidal neurons depends on neurotransmitter release probability. *Proc Natl Acad Sci USA* 94: 719-723, 1997.

Tsodyks M, Uziel A, and Markram H. Synchrony Generation in Recurrent Networks with Frequency-Dependent Synapses. *J Neurosci* 20: 1-5, 2000.

Varela J, Song S, Turrigiano G, and Nelson S. Differential depression at excitatory and inhibitory synapses in visual cortex. *J Neurosci* 19: 4293-4304, 1999.

Williams TL. Phase coupling by synaptic spread in chains of coupled neuronal oscillators. *Science* 258: 662-665, 1992.

Young RE. Neuromuscular control of ventilation in the crab *Carcinus maenas*. *J Comp Physiol A* 101: 1-37, 1975.

Figure Legends

Figure 1. *The Oscillator-Follower model with a depressing synapse.* Neuron O makes a depressing, inhibitory synapse onto a follower neuron F. Top trace shows the membrane potential time courses of neuron F when neuron O is modeled as a square wave oscillator that steps from a low voltage of -50 mV (the inactive state) to a high voltage of +50 mV (the active state). The durations of the active and inactive states, represented as black rectangles and the intervals between them, are defined as T_A and T_I, respectively (bottom). Middle traces are time courses of the synaptic variable *s* (thick line) and the depression variable *d* (thin line). At the instant that O switches from its inactive to its active state, *s* is set to the value of *d*. The time constants that govern the growth and decay of *s* and *d* are indicated.

Figure 2. *The effect of a depressing and a non-depressing synapse on the activity time of the follower neuron, as cycle period varies.* Voltage traces of the follower neuron F when the synapse is non-depressing (thin lines) or depressing (thick lines), at 3 different cycle periods: P = 750 ms (top traces), P = 1000 ms (middle traces), P = 1250 ms (bottom traces). P was modified by changing the duration of the inactive state of O. Rectangles represent the duration of the active state of O (black), the time interval from the end of the active state of O to the beginning of the active state in F when the synapse is depressing (yellow) or non-depressing (magenta).

Figure 3. *Cycle period was modified using three different methods.* Schematic diagrams represent the activity of neuron O, which alternated between a high voltage of +50 mV

(black rectangles) and a low voltage of -50 mV (white rectangles). In the constant T_A case (top), P was varied by changing the duration T_I of the inactive state. In the constant DC case (middle), P was varied by changing T_A and T_I proportionally, such that the duty cycle $DC = T_A/(T_I + T_A)$ remained constant. In the constant T_I case (bottom), cycle period was varied by changing the duration T_A of the active state.

Figure 4. *Dependence of synaptic conductance on cycle period, when cycle period is changed by keeping either T_A, DC or T_I constant.* **A**. Voltage of F and synaptic conductance are shown versus time at P = 500 ms (left), 1000 ms (middle) and 2000 ms (right), when the duration T_A of the active state of O (black rectangles) is fixed at 250 ms. **B.** g_{peak} and g_{jump} as function of P. $\bar{g}_{syn}$ and g^* mark the maximal synaptic conductance, and the synaptic conductance below which the synapse is too weak to keep F in its inactive state, respectively. **C, D.** same as **A** and **B**, when DC (ratio of T_A to P) is fixed at 0.3. **E, F.** same as **A** and **B**, when T_I (intervals between black squares) is fixed at 750 ms.

Figure 5. *Dependence of Δt and ϕ on cycle period in the constant T_A case.* Intervals of activity in O (black rectangles) had a fixed duration (T_A) of 250 ms. **A**. Voltage of F (top traces) and synaptic conductance (bottom traces) at P = 1000 ms (left) and P =2000 ms (right), when the synapse was depressing (solid traces) and non-depressing (dotted traces). **B, C.** Plot of Δt vs. P and ϕ vs. P when the synapse was depressing (black) and non-depressing (blue). The parameter $\bar{g}_{syn}$ of the non-depressing case was tuned to obtain ϕ = 1 at P = 500 ms. The red curves show the idealized case of phase constancy ϕ =

0.643 (the phase of the depressing case when P = 500 ms). Vertical dotted lines in **C** mark the 1-second interval 500 ms ≤ P ≤ 1500 ms.

Figure 6. *Dependence of Δt and ϕ on cycle period in the constant DC case.* **A**. Voltage of F (top traces) and synaptic conductance (bottom traces) at P = 1000 ms (left) and P =2000 ms (right), when the synapse was depressing (solid traces) and non-depressing (dotted traces). Black rectangles represent the intervals of activity in O. The duty cycle DC (ratio of T_A to P) had a fixed value of 0.3. **B, C.** Plot of Δt vs. P and ϕ vs. P when the synapse was depressing (black curves), weak non-depressing (blue curves, $\overline{g}_{syn}$ tuned to match the depressing case at P = 500, 1000 and 2000 ms, curves 1, 2 and 3, respectively) and strong non-depressing (green curves, $\overline{g}_{syn}$ tuned to obtain ϕ = 1 at P = 500 ms). The red curves show the idealized case of phase constancy ϕ = 0.437 (the phase of the depressing case at P = 500 ms). Vertical dotted lines in **C** mark the 1-second interval 500 ms ≤ P ≤ 1500 ms

Figure 7. *Dependence of Δt and ϕ on cycle period in the constant T_I case.* **A**. Voltage of F (top traces) and synaptic conductance (bottom traces) at P = 1000 ms (left) and P =2000 ms (right), when the synapse was depressing (solid traces) and non-depressing (dotted traces). Black rectangles represent the intervals of activity in O. Duration T_I of the inactive state in O had a fixed value of 750 ms. **B, C.** Plot of Δt vs. P and ϕ vs. P when the synapse was depressing (black curves), weak non-depressing (blue curves, $\overline{g}_{syn}$ tuned to match the depressing case at P = 3000 ms, curve 2; curves 3 and 1 were obtained by doubling or halving the maximal conductance used for curve 2) and strong non-

depressing (green curves, $\bar{g}_{syn}$ tuned to match the depressing case at P = 800 ms). The red curves show the idealized case of phase constancy ϕ = 0.491 (the phase of the depressing case at P = 800 ms). Vertical dotted lines in **C** mark the 1-second interval 800 ms $\leq P \leq$ 1800 ms

Figure 8. *The effect of intrinsic and synaptic parameters on the phase-period curve in the constant T_A case.* All panels show phase vs. period when the synapse was depressing and T_A was fixed at 250 ms, at different parameter values. The thick curves denote the reference model (see Methods). Values for reference model are italicized. **A.** Maximal synaptic conductance $\bar{g}_{syn}$ was set to (in mS/cm^2, from top to bottom): 0.225, 0.205, *0.185*, 0.165 or 0.145. **B.** Time constant of recovery τ_α was set to (in ms, from top to bottom): 1500, 2250, *3000*, 3750 and 4500. **C.** Time constant of decay τ_κ was set to (in ms, from top to bottom): 3000, 2250, *1500*, 750 and 375. **D.** Time constant τ_F of intrinsic dynamics in F was set to (in ms, from top to bottom): 250, 200, *150*, 100 and 50.

Figure 9. *The effect of intrinsic and synaptic parameters on the phase-period curve in the constant DC case*. All panels show phase vs. period when the synapse was depressing and *DC* was fixed at 0.3, at different parameter values. The thick curves denote the reference model (values below are italicized). **A.** Maximal synaptic conductance $\bar{g}_{syn}$ was set to (in mS/cm^2, from top to bottom): 0.26, 0.24, *0.22*, 0.2 or 0.18. **B.** Time constant of recovery τ_α was set to (in ms, from top to bottom): 1500, 2250, *3000*, 3750 and 4500. **C.** Time constant of decay τ_κ was set to (in ms, from top to bottom): 1000, 750,

500, 250 and 125. **D.** Time constant τ_F of intrinsic dynamics in F was set to (in ms, from top to bottom): 200, 150, *100*, 50 and 25.

Figure 10. *The effect of intrinsic and synaptic parameters on the phase-period curve in the constant T_I case*. All panels show phase vs. period when the synapse was depressing and T_I was fixed at 750 ms, at different parameter values. The thick curves denote the reference model (values italicized). **A.** Maximal synaptic conductance $\bar{g}_{syn}$ was set to (in mS/cm^2, from top to bottom): 0.55, 0.45, *0.35*, 0.25 or 0.15. **B.** Time constant of recovery τ_α was set to (in ms, from top to bottom): 1500, 2250, *3000*, 3750 and 4500. **C.** Time constant of decay τ_κ was set to (in ms, from top to bottom): 600, 450, *300*, 150 and 75. **D.** Time constant τ_F of intrinsic dynamics in F was set to (in ms, from top to bottom): 200, 150, *100*, 50 and 25.

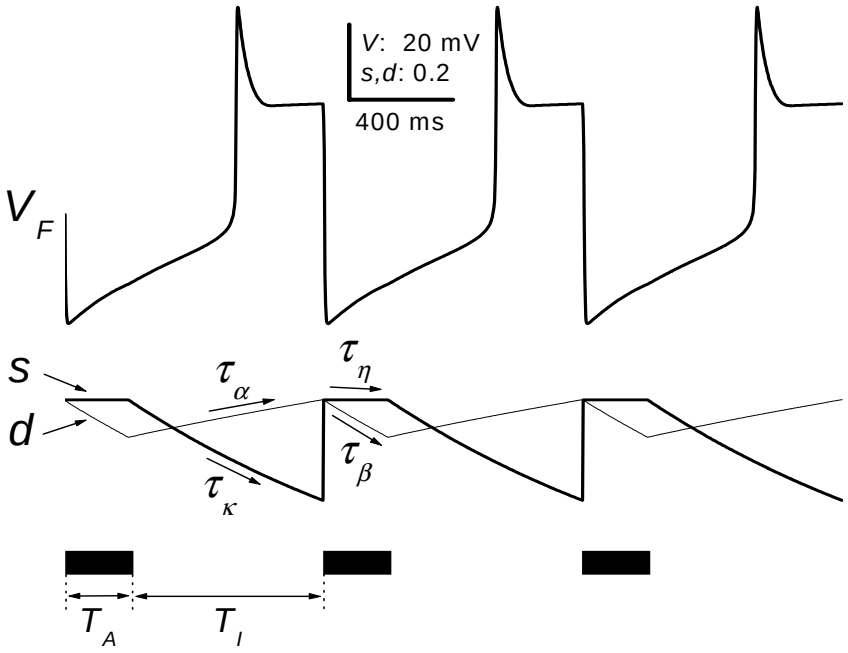
V: 20 mV
s,d: 0.2
400 ms
V_F
s
d
τ_α
τ_η
τ_κ
τ_β
T_A
T_I

Figure 1

Figure 2

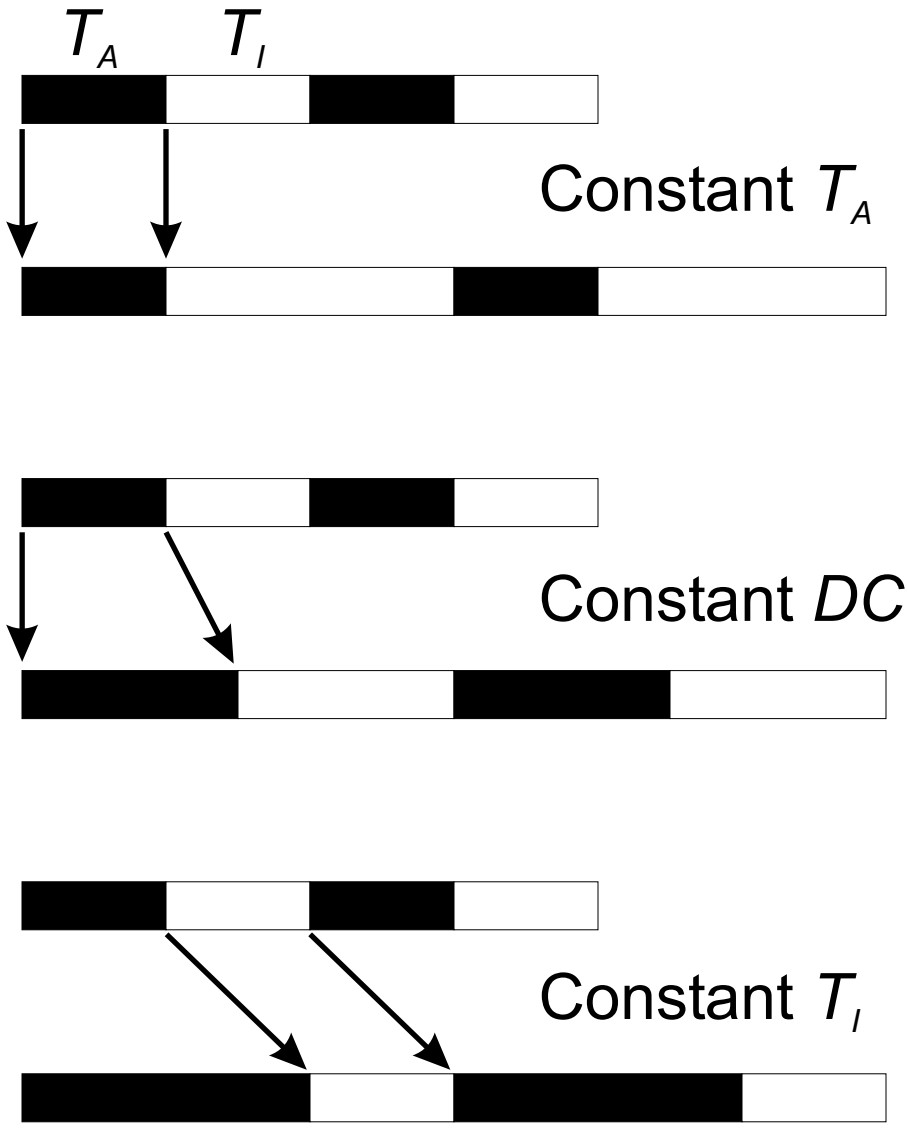

Figure 3

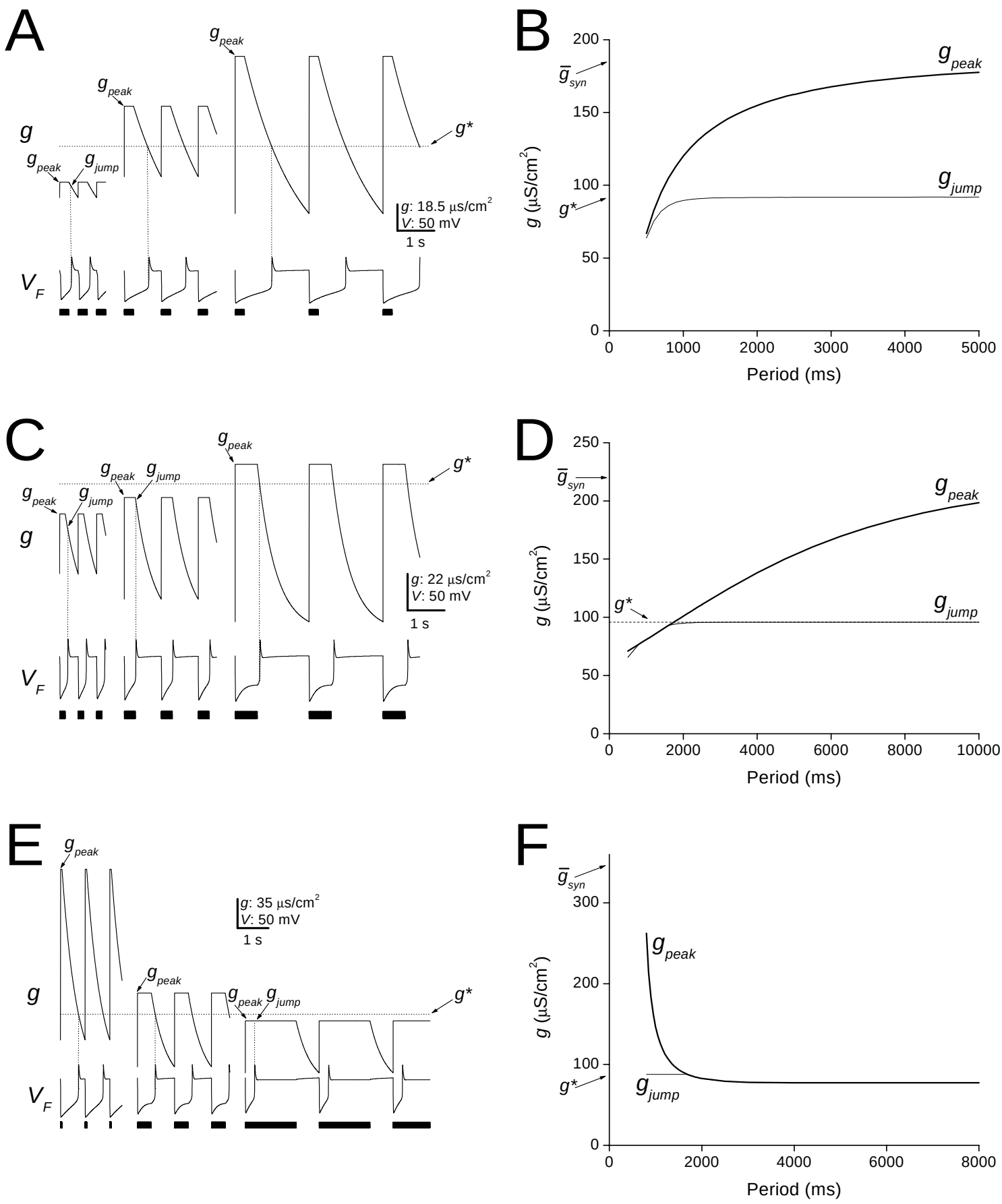
A
B
C
D
E
F
g
V_F
g_peak
g_jump
g*
g: 18.5 µs/cm²
V: 50 mV
1 s
g: 22 µs/cm²
V: 50 mV
g: 35 µs/cm²
V: 50 mV
ḡ_syn
g (µS/cm²)
Period (ms)
0
50
100
150
200
250
300
1000
2000
3000
4000
5000
6000
8000
10000

Figure 4

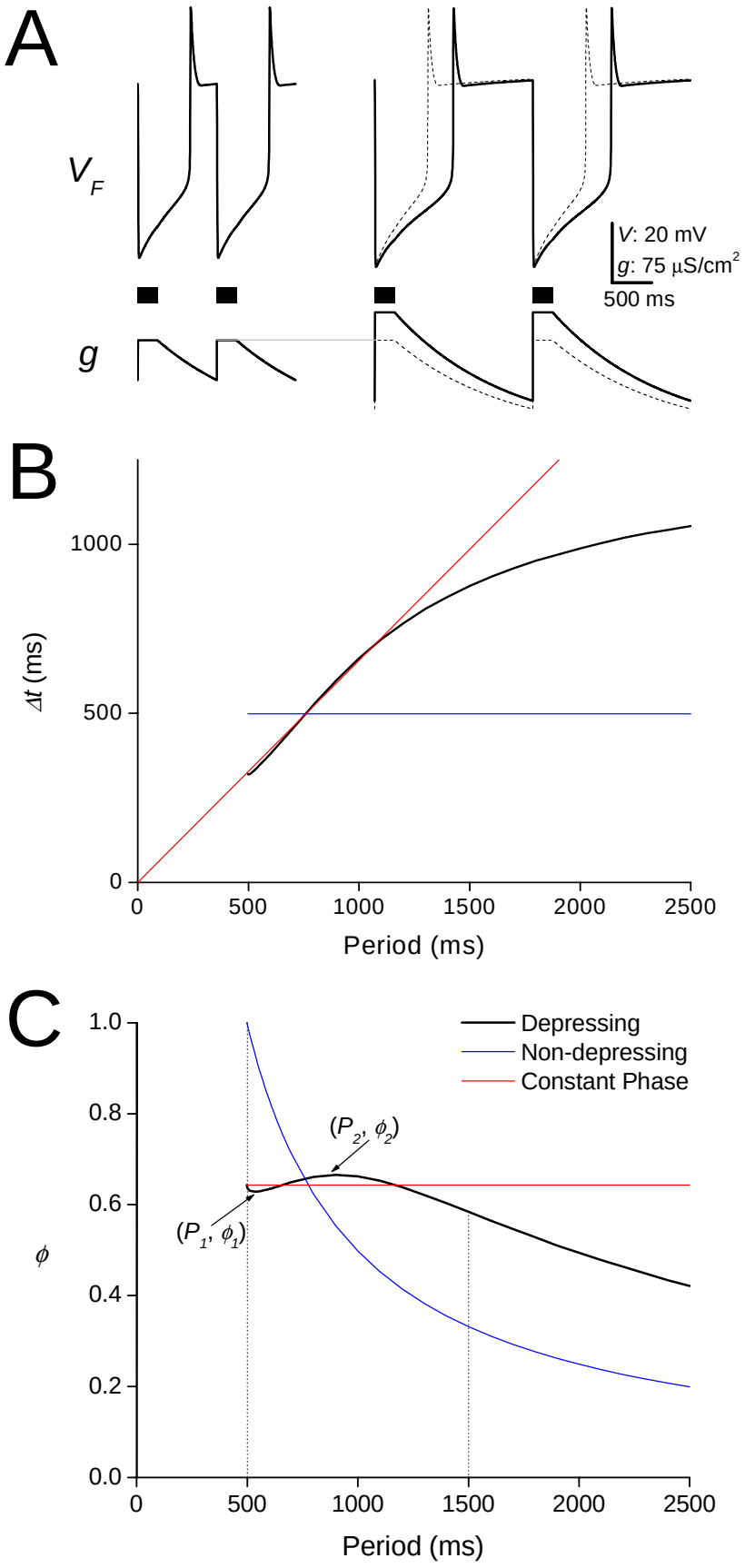
A
V_F
V: 20 mV
g: 75 μS/cm²
500 ms
g
B
1000
500
0
Δt (ms)
0
500
1000
1500
2000
2500
Period (ms)
C
1.0
0.8
0.6
0.4
0.2
0.0
ϕ
Depressing
Non-depressing
Constant Phase
(P2, ϕ2)
(P1, ϕ1)
0
500
1000
1500
2000
2500
Period (ms)

Figure 5

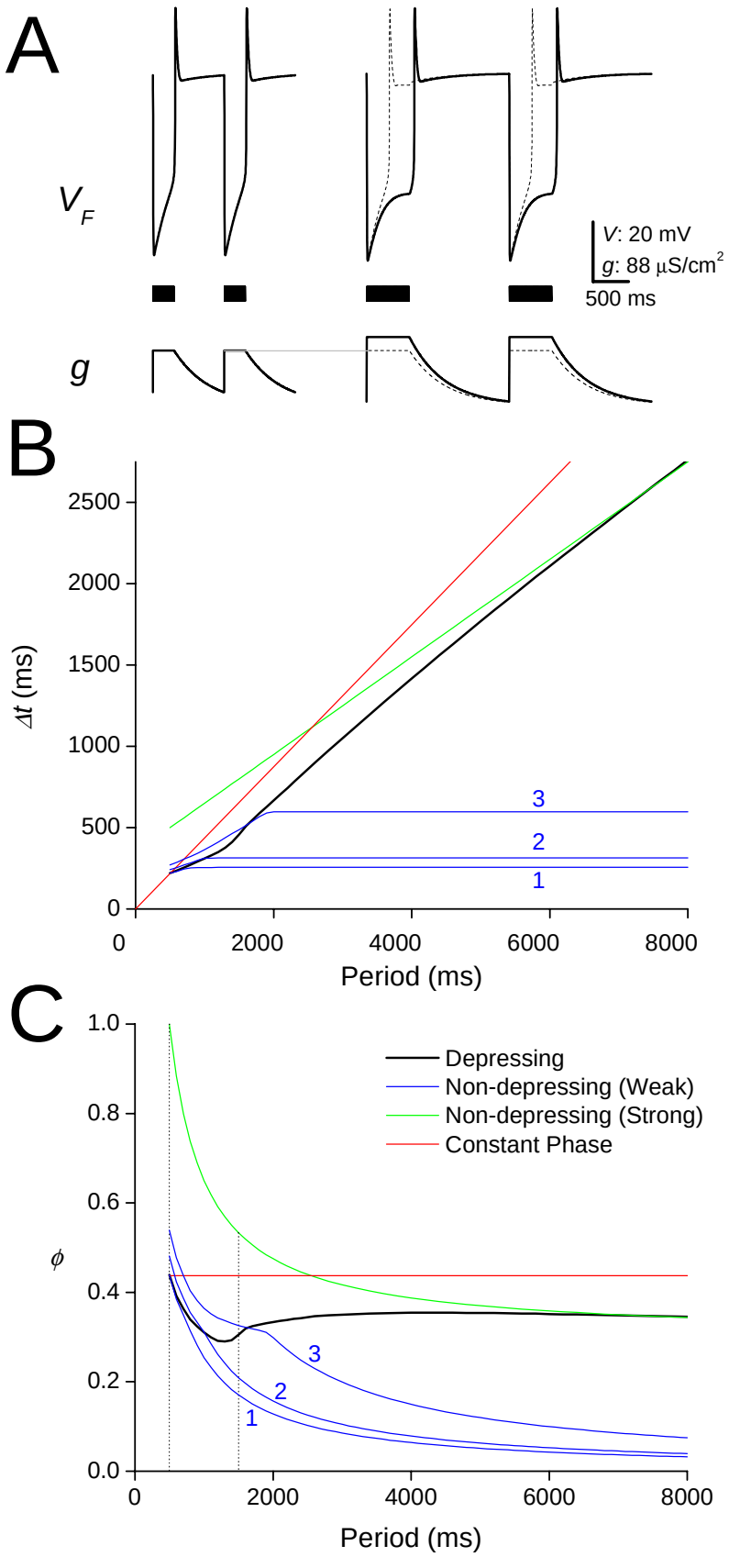
A
V_F
V: 20 mV
g: 88 μS/cm^2
500 ms
g
B
Δt (ms)
2500
2000
1500
1000
500
0
0
2000
4000
6000
8000
Period (ms)
3
2
1
C
ϕ
1.0
0.8
0.6
0.4
0.2
0.0
0
2000
4000
6000
8000
Period (ms)
Depressing
Non-depressing (Weak)
Non-depressing (Strong)
Constant Phase
3
2
1

Figure 6

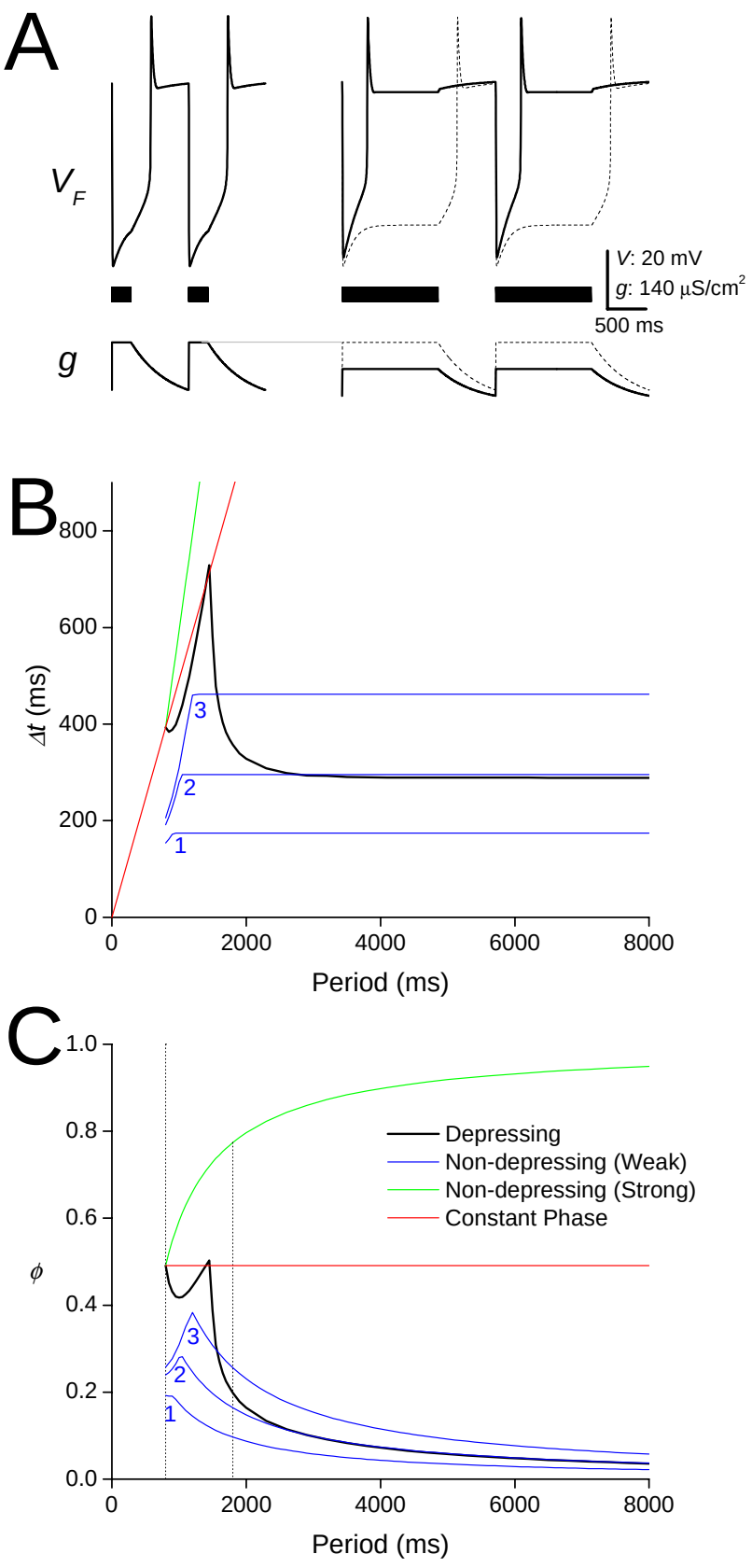
A
V_F
g
V: 20 mV
g: 140 μS/cm^2
500 ms
B
Δt (ms)
Period (ms)
1
2
3
C
ϕ
Period (ms)
Depressing
Non-depressing (Weak)
Non-depressing (Strong)
Constant Phase

Figure 7

Constant T_A

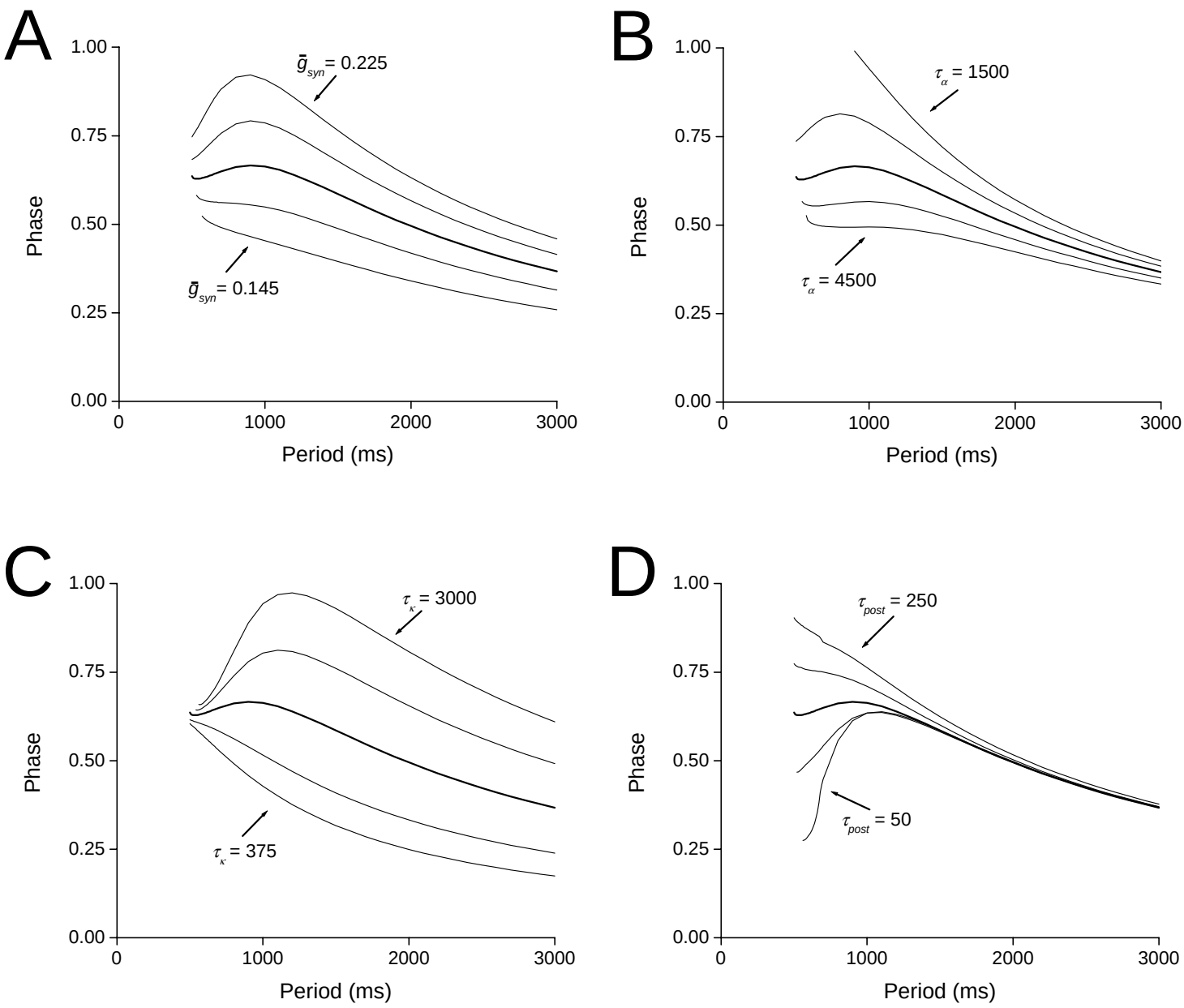

Figure 8

Constant Duty Cycle

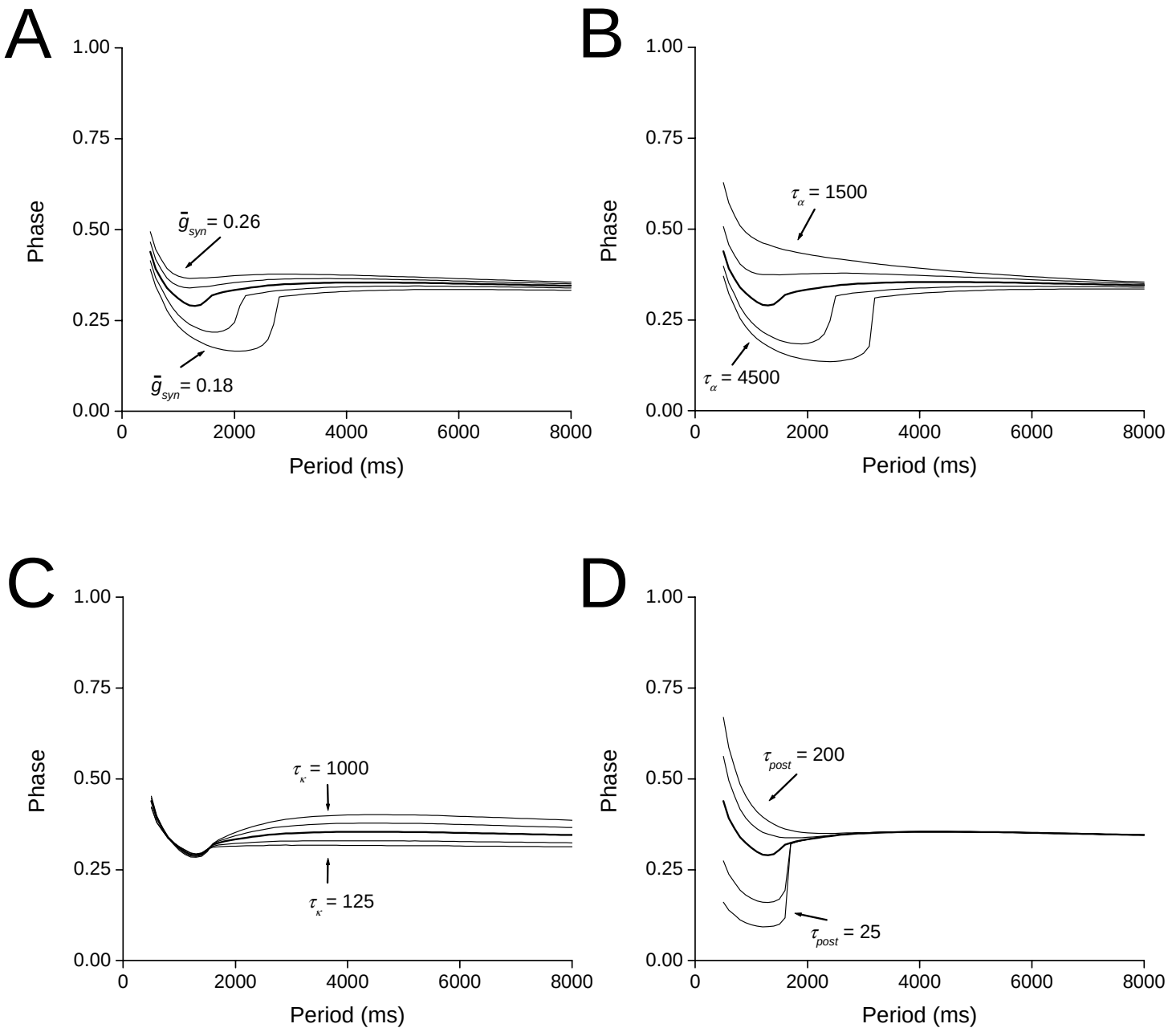

Figure 9

Constant T_I

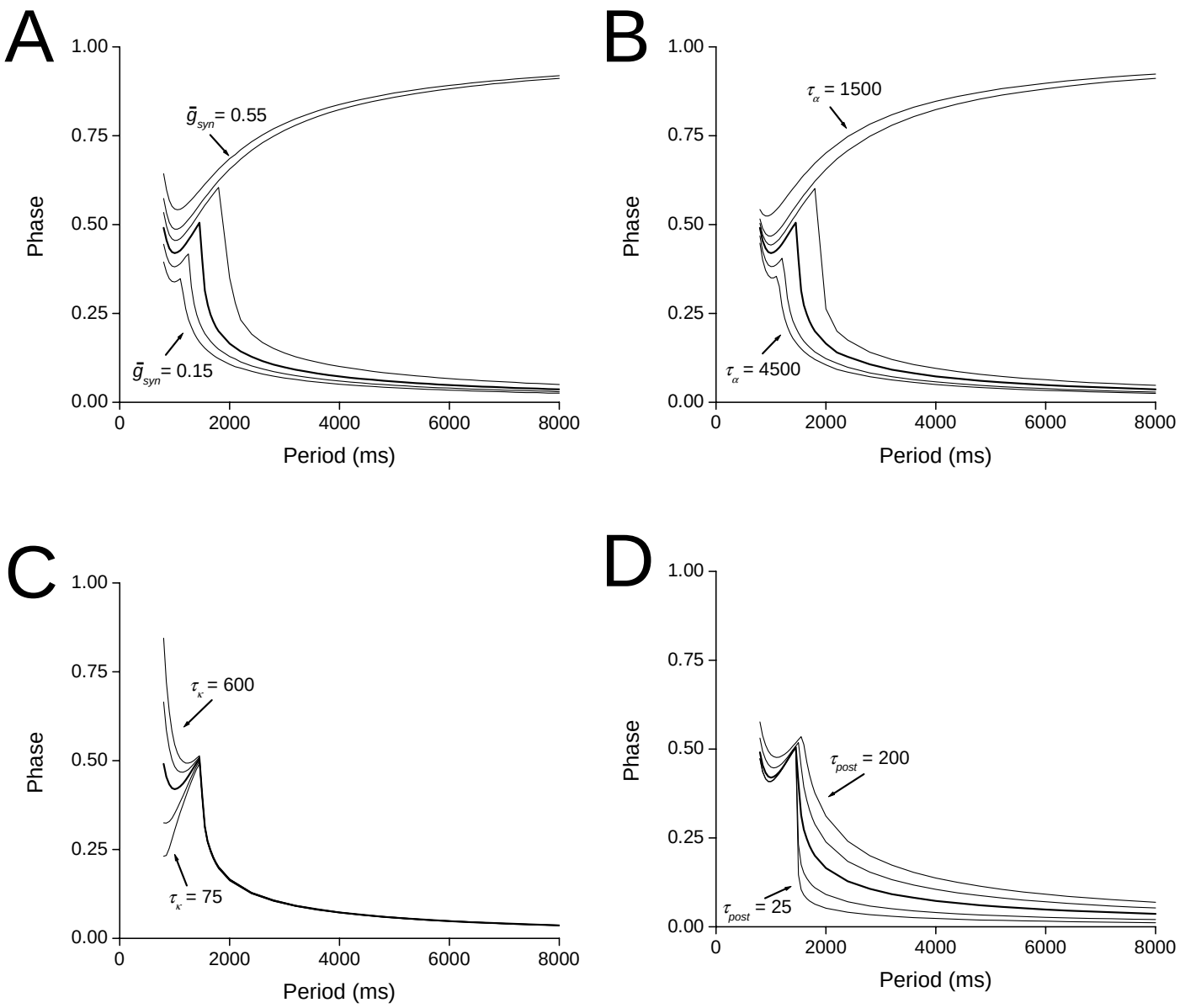

Figure 10